

Asymmetric Pt/Co/Pt-stack induced sign-control of current-induced magnetic domain-wall creep

R. Lavrijsen,^{a)} P. P. J. Haazen, E. Murè, J. H. Franken, J. T. Kohlhepp, H. J. M. Swagten, and B. Koopmans

Department of Applied Physics, Center for NanoMaterials and COBRA Research Institute, Eindhoven University of Technology, P.O. Box 513, 5600 MB Eindhoven, The Netherlands

(Received 13 May 2012; accepted 14 June 2012; published online 28 June 2012)

We report experimentally obtained magnetic domain wall (DW) velocities of current-assisted field-driven DW creep in perpendicularly magnetized Pt/Co/Pt. We have *intentionally* introduced an asymmetry in the stacks by using *different* thicknesses of the two Pt layers sandwiching the Co layer. Thereby, it is tested whether conflicting current-induced domain wall motion (CI-DWM) results may be intrinsically related to the basic layout and growth. We sketch a scenario which could be at the basis of contradicting reports in literature where the direction of CI-DWM conflicts with spin-torque-transfer theory, allowing the sign of the current-induced effect on DW motion to be tuned. © 2012 American Institute of Physics. [<http://dx.doi.org/10.1063/1.4732083>]

Manipulation of the magnetization of ferromagnets through torques induced by spin-polarized currents is a rapidly evolving research field. This is due to the prospect of devices with reduced size and energy consumption.^{1,2} An actively investigated topic is current-induced domain wall motion (CI-DWM)^{3–5} in perpendicularly magnetized materials.^{5–8} These materials exhibit narrow and simple Bloch-type domain walls (DWs) predicted to enhance the interaction with spin-polarized currents.^{9–11} The archetypal material for CI-DWM in perpendicularly magnetized materials are Pt/Co (multi)-layers. Over the last years, many experimental reports have appeared on the CI effects on DWM (Refs. 5–8) in these systems, and even prototype DW shift registers have been demonstrated.¹² There are, however, fundamental contradicting results between the experimental observations and the predictions from theory behind the spin-transfer-torque (STT) used to explain CI-DWM. Using simple macroscopic arguments based on approximate spin conservation one expects that the DW always moves in the direction of the spin current, which, in the case of positive spin polarization, would be against the electrical current and with the flow of electrons.^{7,13} There are, however, conflicting reports where the CI-DWM motion is, very surprisingly, in the direction of the electrical current.^{8,12,14,15} A possible explanation could be a negative spin-polarization.¹⁶ However, this would mean that the spin-polarization varies strongly between nearly identical material systems which is very unlikely.

To address these issues we studied CI-DWM in Pt/Co/Pt stacks by intentionally varying the Pt layer thicknesses. Our experiment showed a decisive role of the Pt/Co/Pt stack geometry, which cannot be understood using the classical STT description of CI-DWM. We will propose that this incoherence can be due to growth-induced irregularities of the Pt/Co interfaces or a completely different interpretation of the phenomenon. Indeed, in the presence of heavy elements like Pt

and/or structural inversion asymmetry, spin-orbit torques can be significant as was, e.g., shown in Pt/Co/AlO_x due to a Rashba field^{8,17–19} and in Ta/CoFeB containing multilayers due to the spin Hall effect.²⁰ We believe that the current experiments will contribute to a further understanding of the origin of DW manipulation in perpendicularly magnetized strips, which in turn is key for future implementation of current-induced magnetization manipulation in spintronics devices.

We have chosen to investigate field-driven current-assisted DW motion in Pt/Co/Pt stacks where we have varied the Pt layer thicknesses: SiO₂//Pt(4)/Co(0.6)/Pt(2), SiO₂//Pt(3)/Co(0.6)/Pt(3), and SiO₂//Pt(2)/Co(0.6)/Pt(4), all thicknesses given in nm. We will from now on label these samples indicating only the Pt layers as Pt₄/Co/Pt₂, Pt₃/Co/Pt₃, and Pt₂/Co/Pt₄, respectively. A typical device is shown in Fig. 1(a), where the Pt/Co/Pt layers are prepared by DC magnetron sputtering on Si substrates with a 100 nm thermally grown SiO₂ layer. The structures are patterned into 900 nm wide strips using electron beam lithography (EBL) and Ar ion milling. The strips are electrically connected with Ti/Au electrodes using EBL and lift-off. The capital letters indicate the components of the device: Contacts indicated by (A) are used to inject an AC (detection) and/or a DC offset current into the magnetic wire. (B) Pulse line electrically isolated from the magnetic wire by a 20 nm thick SiO₂ layer (dark square). The pulse line is used to create a DW in the magnetic strip by the Oersted field of a large injected current pulse. (C) 10 nm thick 1 μm wide Pt lines spaced 20 μm apart on top of the magnetic strip, locally probing the magnetization state of the strip by the anomalous Hall effect. The devices are placed in a He-flow cryostat where the temperature is actively controlled to $T = 300 \pm 1$ K. The procedure to measure the DW velocity can be found in Ref. 21. The current density J is determined by dividing the injected DC current into the strip by the cross-sectional area of the wire.

Having different Pt thicknesses above and below the Co-layer but keeping the total stack thickness constant will allow us to investigate the effect of structural asymmetry on current-induced effects. In Figs. 1(b)–1(d), these samples are

^{a)}Present address: Cavendish Laboratory, University of Cambridge, JJ Thompson Avenue, Cambridge CB3 0HE, United Kingdom. Electronic mail: r1433@cam.ac.uk.

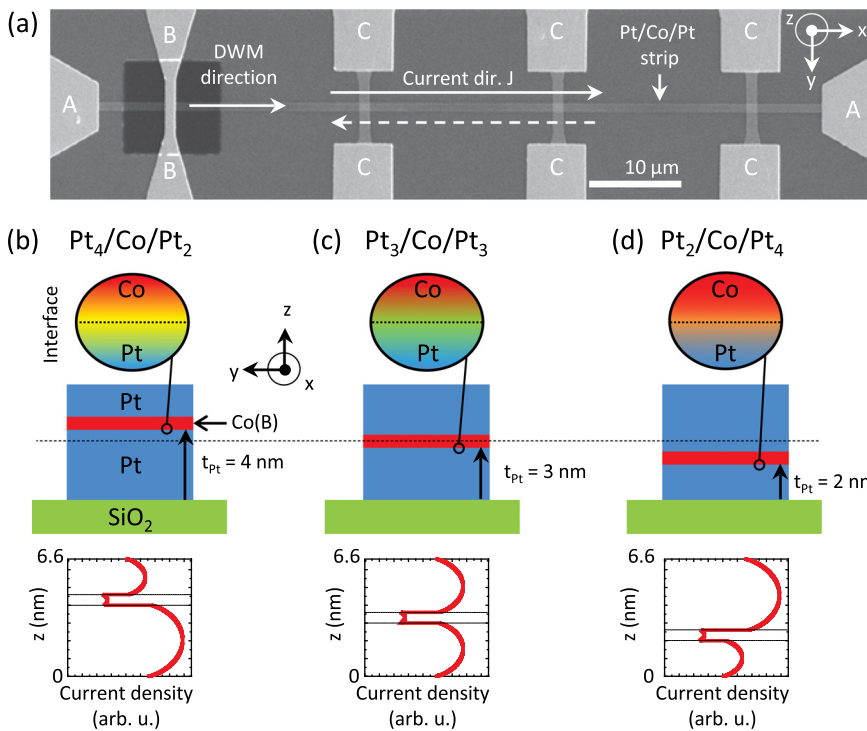


FIG. 1. (a) Typical device used for all measurements (see text). (b)–(d) Schematic illustrations of the used layers stacks, the different Pt/Co interface qualities depending on the bottom Pt layer thickness and calculated current-density distributions in the stacks.

schematically illustrated together with two direct consequences of this approach. First, the different bottom Pt thicknesses, grown directly on the substrate, result in a different interface quality with the Co layer,^{22,23} schematically illustrated by the different colors at the Pt/Co interface. Second, when a current is passed through such a tri-layer stack a different current density distribution is expected. We calculated the distribution for our stacks using the model of Cormier *et al.*²⁴ and the results are shown below the stack-illustrations. We will refer to these scenarios when discussing the experimental results.

In Figs. 2(a)–2(c), the average DW velocity \bar{v} as a function of drive field H_z is shown for different current densities $J=0$ (black), $J=3.4 \times 10^{11}$ (blue), and $J=5.1 \times 10^{11}$ (red) A/m² and current directions. Every point is the average of 20 measurements, the error bars indicate the standard deviation. The high perpendicular magnetic anisotropy of the Pt/Co/Pt layers leads to narrow Bloch DWs which are easily pinned at structural inhomogeneities. This leads to the well-known thermally assisted DW creep motion: $\log(\bar{v}) \propto H_z^{-1/4}/(k_B T)$ at low H_z , where $k_B T$ is the thermal energy.²⁵ Hence, when $\log(\bar{v})$ is plotted versus $(\mu_0 H_z)^{-1/4}$ one expects a linear dependence as is seen in Fig. 2. The deviation from a linear behavior at high H_z and J is attributed to a transition to the so-called flow regime where the creep-scaling is no longer valid.²⁶ Note that with decreasing bottom Pt thickness, a lower H_z is needed to drive the DWs with an identical velocity indicating a decreasing pinning strength for a thinner bottom Pt layer. On injecting a current, we observe that the overall DW velocity increases. This is primarily due to Joule heating increasing the thermally assisted DWM.

What is surprising, however, is that we observe a different increase in \bar{v} for *identical* current densities but with *opposite* polarity. In the case of Pt₄/Co/Pt₂ [Fig. 2(a)], the

increase in DW velocity is higher when the current flows *in the same direction* as the DWM (filled symbols). On the contrary, in Pt₂/Co/Pt₄ [Fig. 2(c)] the DW velocity increase is higher when the current flow is *opposing* the DWM (open symbols). Moreover, in the symmetric Pt₃/Co/Pt₃ sample [Fig. 2(b)] the difference is small. Apparently, there should be an additional CI-DWM effect since the conventional STT alone cannot explain the CI-sign change between Pt₄/Co/Pt₂ and Pt₂/Co/Pt₄.

To rule out the effect of an Oersted field, we have performed identical measurements but now we only reverse the magnetic drive field direction $\mu_0 H_z$. If the z -component of the Oersted fields of the injected DC currents would be responsible for the effect, we would expect that on reversing the drive field direction the observed current-assisted DW velocity enhancement would also change. In Fig. 3, we show the average DW velocity as a function of current density $|J|$ for constant $|\mu_0 H_z| = 21$ mT for both polarities in Pt₄/Co/Pt₂. Again, we can see the overall velocity increases with current density as attributed to Joule heating. However, for both drive field directions, the DW moves faster when the current is flowing in the direction of DWM indicating that the Oersted fields cannot be responsible for the observed sign change. The y -component of the Oersted field has been calculated using finite element calculations in COMSOL with as input the current density distributions as shown in Figs. 1(b)–1(d) with an integrated total current density as in the experiments. The maximum field at the magnetic layer was calculated to be ≈ 1 mT. We have verified that such a H_y field cannot explain the observed behavior using a simple one-dimensional DW (1D) model and full micro-magnetic simulations.

To rule out any temperature effects as a cause of the effect we have performed constant sample temperature measurements. In these measurements, we measure the

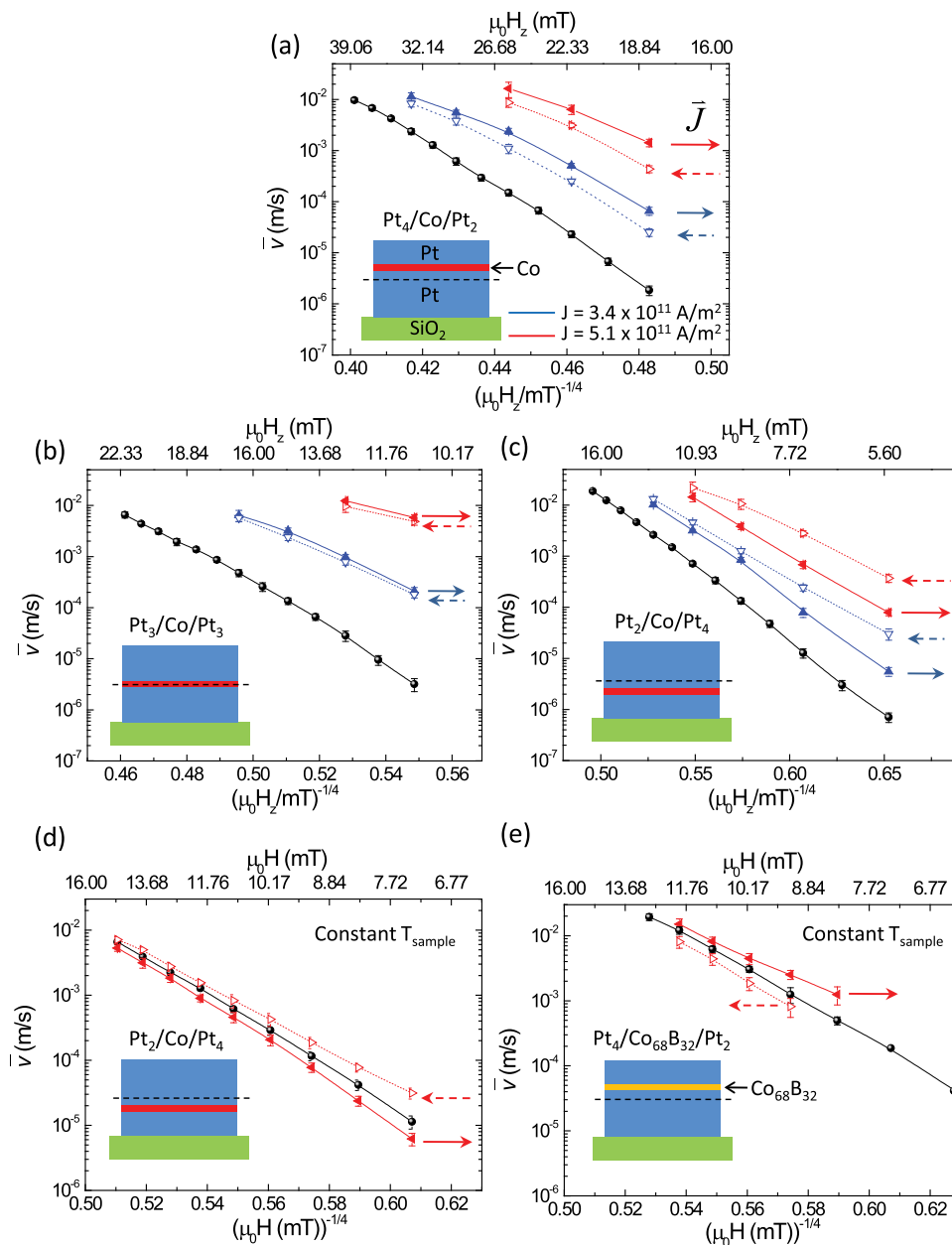


FIG. 2. Average DW velocity of 20 measurements plotted as a function of applied field for ($J = 0, \pm 3.4 \times 10^{11}, \pm 5.1 \times 10^{11} \text{ A/m}^2$), the error bars indicate the standard deviation. Results obtained in: (a) Pt₄/Co/Pt₂, (b) Pt₃/Co/Pt₃, (c) Pt₂/Co/Pt₄, (d) Pt₂/Co/Pt₄ with constant sample temperature, and (e) Pt₄/Co₆₈B₃₂/Pt₂ with constant sample temperature. The blue and red filled symbols/solid line (open symbols/dashed line) correspond to the current flowing with (against) the direction of DWM, to the right, as indicated by the arrows in Fig. 1(d). Note that the top-axis scale is non-linear.

increase in temperature due to the injected current by relating the resistance increase (4-point) due to the injected DC current J to the temperature dependence of the resistance. We compensate for this temperature rise by cooling down the cryostat; for the details of the experiment we refer to Boulle *et al.*⁶ The result is shown in Fig. 2(d) for Pt₂/Co/Pt₄. We observe that the DW velocity either increases or decreases symmetrically relative to the purely field driven case ($J=0$), which unambiguously shows that the CI-effect changes sign relative to the pure field-driven DWM ($J=0$), inline with earlier observations. The result is the same for the Pt₄/Co/Pt₂ structure (not shown) but with reversed polarity, i.e., now the positive current increases the DW velocity, as was seen in Fig. 2.

As seen in Fig. 2, there is a lower DW pinning strength in Pt₂/Co/Pt₄ compared to Pt₄/Co/Pt₂, i.e., a lower drive field H_z is needed for an identical DW velocity due to the different bottom Pt thicknesses giving different pinning strengths.^{22,23} To show that this difference in DW pinning

strength is not responsible for the observed change in the STT we have performed constant sample temperatures DW velocity measurements on a Pt₄/Co₆₈B₃₂/Pt₂ sample. This sample has the same Pt layer asymmetry as Pt₄/Co/Pt₂ but a strongly reduced DW pinning due to the boron doped (32 at. %) Co.²⁷ The results are shown in Fig. 2(e), where we indeed observe a similar CI-sign behavior as in Pt₄/Co/Pt₂, i.e., the DW velocity increases when the current flows in the same direction as the DWM indicated by the arrows. Hence, we conclude that the DW pinning strength is not the cause of the CI-sign change between Pt₄/Co/Pt₂ and Pt₂/Co/Pt₄, and therefore should have a different origin.

When one compares our stacks with inverted Pt thickness, one should realize that based on symmetry arguments only, there is no basic difference between the two configurations: a DW moving from left to right in a Pt₄/Co/Pt₂ by field and current should in principle have the same DW speed when it is moving from right to left in the structurally inverted Pt₂/Co/Pt₄ when changing field and current

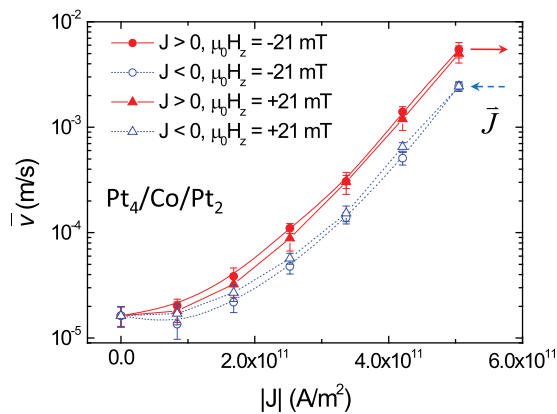


FIG. 3. Average DW velocity as a function of current density $|J|$ for constant $|\mu_0 H_z| = 21$ mT for both polarities of the $\text{Pt}_4/\text{Co}/\text{Pt}_2$ sample.

direction. This means that the present results of a change in CI-sign change between $\text{Pt}_4/\text{Co}/\text{Pt}_2$ and $\text{Pt}_4/\text{Co}/\text{Pt}_2$ could be related to growth-induced differences which are lifting the structural inversion symmetry of the two systems. In turn, these growth-induced effects are then responsible for altered interface regions underneath and on top of the cobalt, or even changes in the magnetization of the cobalt itself, all affecting the spin-current-induced torques acting on the local Co magnetization in a CI-DWM experiment. Following these arguments, the sign change between positive and negative contributions to the CI-DWM then incidentally takes place at a Pt bottom layer thickness of around ~ 3 nm, as shown by the data in Fig. 2(b).

However, recent reports on CI-effects in $\text{Pt}/\text{Co}/\text{AlO}_x$ and $\text{Pt}/\text{Co}/\text{Al}$ evidenced that the strong spin-orbit coupling in the Pt layer is responsible for a torque on the Co magnetization. The origin of this effect is still under debate, and can be due to either the Rashba-torque¹⁹ at the Pt/Co interface or the spin Hall current²⁰ injected from the Pt layers. In these reports, it is shown that the resulting torque tends to stabilize the up (down) orientation of the magnetization, depending on the sign of the current and of the magnetization projection on the direction of the current (x-axis in our reference system, see Fig. 1(a)).

In our structures, due to the presence of a bottom and top Pt layer, there are two competing sources of spin-orbit torque. This would result in different spin-orbit torque amplitude from the bottom and top layer, and net non-zero torque on the magnetization. Further support for the interpretation of using the spin-orbit torque can be found by looking at the current distribution in the Pt/Co/Pt stacks as calculated in Fig. 1. Relating this to our asymmetric $\text{Pt}_4/\text{Co}/\text{Pt}_2$ and $\text{Pt}_2/\text{Co}/\text{Pt}_4$ stacks the spin-orbit torque of the thicker Pt layer would then be dominating over the thinner Pt layer and in the symmetric $\text{Pt}_3/\text{Co}/\text{Pt}_3$ the effective spin-orbit torque would cancel. This would qualitatively explain the results presented in Fig. 2, where we find a CI-sign change between $\text{Pt}_4/\text{Co}/\text{Pt}_2$ and $\text{Pt}_2/\text{Co}/\text{Pt}_4$ and no effect in $\text{Pt}_3/\text{Co}/\text{Pt}_3$.

Based on a spin-orbit torque interpretation on the CI-DWM, we will now try to shed light on the discrepancy in literature where CI-DWM is either in the direction of current or opposing the electric current direction. The discrepancy can be explained by taking into account the buffer layers

below and above the magnetic layer(s). For example, in a $\text{Ta}(5)/\text{Pt}(2.5)/\text{Co}(0.3)/\text{Pt}(1.5)$ stack^{12,15} with a thicker underlayer, pure CI-DWM is observed to be in the direction of current corresponding to our $\text{Pt}_4/\text{Co}/\text{Pt}_2$. In the case of $\text{Pt}(2.8 \text{ nm})/\text{Co}(0.5 \text{ nm})/\text{Pt}(1.0)/\text{Co}(0.5)/\text{Pt}(1.0)$,⁷ the field driven DW-creep is more efficient when the current opposes the DWM direction in-line with the current belief that the CI-DWM is in the direction of the electron flow. One could argue that their stack is asymmetric in the thickness of the Pt layers relative to the two Co layers, similar to the previous case, but the situation is more complicated due to the multi-layered stack where the magnetization in the two layers is coupled.²⁸ The experiments on $\text{Pt}/\text{Co}/\text{AlO}_x$ (Refs. 8, 17–19) showed that CI-DWM is in the direction of current flow which is qualitatively in line with our observations in $\text{Pt}_4/\text{Co}/\text{Pt}_2$. $\text{Pt}_4/\text{Co}/\text{Pt}_2$ has a similar stack-asymmetry as $\text{Pt}/\text{Co}/\text{AlO}_x$ leading to a concentrated current in the bottom Pt layer/bottom interface. From the discussion above, it is clear that no firm conclusions can be drawn when comparing the direction of CI-DWM between our present data and the (limited) reports available in literature. However, the overall trends we have indicated do seem to support our conjecture that a specific (a)symmetry in stacking these perpendicular materials is key to the experimental observations. We hope that this work may initiate further experimental and theoretical work to unravel the detailed origin of these intriguing sign changes in domain-wall motion.

We reported the experimental observation of field-driven current-assisted DWM. Surprisingly, the DW velocity as function of field and current depends on the (a)symmetry of the Pt/Co/Pt stack by changing the thickness of the bottom and top Pt layer, and is discussed in terms of the induced structural inversion (a)symmetry related to growth and/or spin-orbit torques. The possibility to tune CI-sign in the current-assisted field-driven DWM in the widely used archetypical perpendicularly magnetized material Pt/Co/Pt will greatly help the interpretation and implementation of current-induced magnetization manipulation in devices based on perpendicular magnetized materials.

We thank NanoNed, a Dutch nanotechnology program of the Ministry of Economic Affairs. E.M. acknowledges support from the Swiss National Science Foundation (SNSF), Grant No. PBELP2-130894. J.H.F. acknowledges support from the Foundation for Fundamental Research on Matter (FOM), which is part of the Netherlands Organization for Scientific Research (NWO).

¹C. Chappert, A. Fert, and F. Nguyen van Dau, *Nature Mater.* **6**, 813 (2007).

²J. Katine and E. Fullerton, *J. Magn. Magn. Mater.* **320**, 1217 (2008).

³M. Kläui, *J. Phys.: Condens. Matter.* **20**, 313001 (2008).

⁴S. S. P. Parkin, M. Hayashi, and L. Thomas, *Science* **320**, 190 (2008).

⁵C. Burrowes, A. Mihai, D. Ravelosona, J.-V. Kim, C. Chappert, L. Vila, A. Marty, Y. Samson, F. Garcia-Sanchez, L. Buda-Prejbeanu, I. Tudosa, E. Fullerton, and J.-P. Attané, *Nat. Phys.* **6**, 17 (2009).

⁶O. Boulle, J. Kimling, P. Warnicke, M. Kläui, U. Rüdinger, G. Malinowski, H. Swagten, B. Koopmans, C. Ulysse, and G. Faini, *Phys. Rev. Lett.* **101**, 216601 (2008).

⁷L. San Emeterio Alvarez, K.-Y. Wang, S. Lepadatu, S. Landi, S. Bending, and C. H. Marrows, *Phys. Rev. Lett.* **104**, 137505 (2010).

⁸I. M. Miron, T. Moore, H. Szabolcs, L. Buda-Prejbeanu, S. Auffret, B. Rodmacq, S. Pizzini, J. Vogel, M. Bonfim, A. Schuhl, and G. Gaudin, *Nature Mater.* **10**, 419 (2011).

- ⁹D. Ravelosona, D. Lacour, J. Katine, B. Terris, and C. Chappert, *Phys. Rev. Lett.* **95**, 117203 (2005).
- ¹⁰S. Zhang and Z. Li, *Phys. Rev. Lett.* **93**, 127204 (2004).
- ¹¹G. Tatara and H. Kohno, *Phys. Rev. Lett.* **92**, 086601 (2004).
- ¹²K.-J. Kim, J.-C. Lee, J.-Y. Sang, G.-H. Gim, K.-S. Lee, S.-B. Choe, and K.-H. Shin, *Appl. Phys. Express* **3**, 083001 (2010).
- ¹³T. Koyama, G. Yamada, H. Tanigawa, S. Kasai, N. Ohshima, S. Fukami, N. Ishiwata, Y. Nakatani, and T. Ono, *Appl. Phys. Express* **1**, 101303 (2008).
- ¹⁴T. A. Moore, I. M. Miron, G. Gaudin, G. Serret, S. Auffret, B. Rodmacq, A. Schuhl, S. Pizzini, J. Vogel, and M. Bonfim, *Appl. Phys. Lett.* **93**, 262504 (2008).
- ¹⁵J.-C. Lee, K.-J. Kim, J. Ryu, K.-W. Moon, S.-J. Yun, G.-H. Gim, K.-S. Lee, K.-H. Shin, H.-W. Lee, and S.-B. Choe, e-print arXiv:1006.1216v1.
- ¹⁶O. Siper, J. Minar, S. Mankovsky, and H. Ebert, *Phys. Rev. B* **78**, 144403 (2008).
- ¹⁷I. M. Miron, P. J. Zermatten, G. Gaudin, S. Auffret, B. Rodmacq, and A. Schuhl, *Phys. Rev. Lett.* **102**, 137202 (2009).
- ¹⁸I. M. Miron, G. Gaudin, S. Auffret, B. Rodmacq, A. Schuhl, S. Pizzini, J. Vogel, and P. Gambarella, *Nature Mater.* **9**, 230 (2010).
- ¹⁹I. M. Miron, K. Garello, G. Gaudin, P. Zermatten, M. V. Costache, S. Auffret, S. Bandiera, B. Rodmacq, A. Schuhl, and P. Gambardella, *Nature (London)* **476**, 189 (2011).
- ²⁰L. Liu, C.-H. Pai, H. W. Tseng, D. C. Ralph, and R. A. Buhrmann, *Science* **336**, 555 (2012).
- ²¹R. Lavrijsen, M. Verheijen, B. Barcones, J. Kohlhepp, H. Swagten, and B. Koopmans, *Appl. Phys. Lett.* **98**, 132502 (2011).
- ²²V. Mathet, T. Devolder, C. Chappert, J. Ferré, S. Lemerle, L. Belliard, and G. Guentherodt, *J. Magn. Magn. Mater.* **260**, 295 (2003).
- ²³A. Adanlété-Adjanoh, R. Belhi, J. Vogel, O. Fruchart, M. Ayadi, and K. Abdelmoula, *J. Magn. Magn. Mater.* **322**, 2498 (2010).
- ²⁴M. Cormier, A. Mougin, J. Ferré, A. Thiaville, N. Charpentier, F. Piéchon, R. Weil, V. Baltz, and B. Rodmacq, *Phys. Rev. B* **81**, 024407 (2010).
- ²⁵P. Chauve, T. Giamarchi, and P. Le Doussal, *Phys. Rev. B* **62**, 6241 (2000).
- ²⁶P. J. Metaxas, J. P. Jamet, A. Mougin, M. Cormier, J. Ferre, V. Baltz, B. Rodmacq, B. Dieny, and R. L. Stamps, *Phys. Rev. Lett.* **99**, 217208 (2007).
- ²⁷R. Lavrijsen, G. Malinowski, J. Franken, J. Kohlhepp, H. Swagten, B. Koopmans, M. Czapkiewicz, and T. Stobiecki, *Appl. Phys. Lett.* **96**, 022501 (2010).
- ²⁸P. J. Metaxas, R. L. Stamps, J.-P. Jamet, J. Ferré, V. Baltz, B. Rodmacq, and P. Politi, *Phys. Rev. Lett.* **104**, 237206 (2010).